DOI: 10.1021/ma902758w

Macromolecules
ARTICLE

Computational Investigation on the Role of Plasticizers on Ion Conductivity in Poly(ethylene oxide) LiTFSI Electrolytes

Hui Wu and Collin D. Wick*

Department of Chemistry, Louisiana Tech University, Ruston, Louisiana 71270

Received December 14, 2009; Revised Manuscript Received March 9, 2010

ABSTRACT: A combination of molecular dynamics and connectivity-altering Monte Carlo simulations was carried out to understand on the molecular level the effect of the addition of plasticizers on lithium ion transport in poly(ethylene oxide) with LiTFSI. The simulations were performed using a moderately high molecular weight polymer (M_n = 10 000 g/mol) mixed with 10 wt % plasticizers at 320 and 348 K at an EO:Li ratio of 15. Comparisons with experiment showed slight underestimation of the ionic conductivity with an array of experimental values, but within a factor of 2 of most. With the addition of ethylene carbonate and propylene carbonate plasticizers, the ionic conductivity increased a moderate degree. However, the lithium diffusion did not show a significant increase with the addition of plasticizers, and most of the conductivity increase was due to faster $TFSI^-$ motion. It was found that propylene carbonate formed complexes with the $TFSI^-$, in which lithium was an intermediary, creating moderate sized clusters. This allowed enhanced diffusion of lithium ions bound with $TFSI^-$ ions, but this was offset by slower diffusion for lithium ions bound with ethylene oxide oxygens. Ethylene carbonate, on the other hand, showed no significant complexing with $TFSI^-$. The formation of these clusters may be an avenue for increasing lithium diffusion but would likely require a plasticizer with stronger interactions with lithium than the carbonates studied.

I. Introduction

The need for energy is one of the greatest challenges facing our country and the world today. Improved electrochemical energy technologies, for instance batteries, will be a key part of the solution to our energy challenges. Rechargeable lithium batteries (RLBs) have been increasingly utilized in consumer electronics and military equipment and have the promise for wide use in electric and hybrid vehicles.[1] However, lithium salts and metals can be highly reactive, making the leakage of liquid electrolytes a major safety concern. Furthermore, at elevated temperatures and in overcharging situations, traditional carbonate electrolytes react with the electrodes, forming gases that cause the batteries to break, resulting in fire or explosion.[2−6] A way to overcome these difficulties is to replace the liquid electrolyte with a polymer electrolyte (PE). PEs have several advantages over liquid electrolytes, including enhanced mechanical properties, ease of fabrication, good electrochemical stability, low flammability, and a reduced propensity for leakage.[7,8] The most widely studied PE is poly(ethylene oxide) (PEO) with lithium salts added to facilitate lithium conduction. The mechanism for lithium transport in PEO has been attributed to the segmental motion of PEO chains.[9] Unfortunately, the ionic conductivity of PEs at room temperature is generally too low for practical use in a battery, being on the order of 10^{-4}−10^{-7} S cm^{-1}, while 10^{-3} or better is needed for viable usage.[1,8,10,11] The low ionic conductivity has been conjectured to be the result of the crystalline nature of PEO near room temperature,[9] even though it has been found that for short-chained PEO crystallinity may enhance conductivity for very specific cases.[12] One common pathway for the enhancement of PE conductivity is to introduce plasticizers, such as cyclic carbonates, which have been shown to enhance the conductivity to practical levels.[13−19] Plasticized polymers are a compromise between the beneficial properties of solid-state PEs and the high conductivities of liquid electrolytes. Despite their importance, little is known about the lithium transport mechanism in these types of PEs on the molecular level.

An understanding of the molecular level details of these systems and how they influence ion motion and conductivity would greatly benefit the design of new PEs and RLBs. Computational methods can bring significant insight into molecular level interactions and structures. Specifically, molecular dynamics (MD) simulations have the benefit of providing a direct picture of the molecular structure but also allow the calculation of macroscopic properties, such as ionic conductivity, which can be directly compared with experiment. This latter step is very important to provide validation for the molecular level observations made. The conduction mechanism for lithium in PEO and in carbonates has been studied extensively by computational methods.[20−39] Investigating ionic conductivity in a system with very high levels of propylene carbonate and some polymer present has been investigated also.[40,41] However, the role of plasticizers on lithium conduction in PEO in low enough concentrations to be relevant for RLBs has not been studied to the knowledge of the authors. It is important to understand exactly how plasticizers affect ionic transport to be able to optimize lithium conductivity in these and similar systems. For instance, do plasticizers significantly change the ion conduction mechanism? What is the influence of plasticizers on the PEO structure? In this work, we report MD simulations, aided by Monte Carlo (MC) simulations for equilibration, of ionic conduction in PEO with the addition of carbonate plasticizers. The paper is organized with simulation details for the MC and MD simulations, along with the molecular models used in section II, results of the work in section III, and conclusions in section IV.

*Corresponding author. E-mail: cwick@latech.edu.

 Published on Web 03/19/2010

II. Simulation Details

II.A. Molecular Models. The majority of the force field parameters used were developed in previous work. The TraPPE-UA force field was used for PEO,[42−44] which utilizes pseudoatoms located at the center of carbon atoms for alkyl groups and treats all other atoms explicitly. This model uses Lennard-Jones (LJ) interactions potentials of the 12−6 form and fixed electrostatic charges. It has been found to do a good job of reproducing PEO densities over a very wide range of temperatures and pressures.[42] The all-atom $TFSI^-$ force field developed by Canongia Lopes and co-workers was also used,[45] and the TraPPE-UA force field was used for the carbonate molecules.[46] While fixed charge Li^+ force fields with LJ interactions exist in the literature,[47] we decided to parametrize a new one that reproduced the binding energy and lithium−oxygen distance with dimethyl ether (DME). *Ab initio* results for interactions between lithium and ether oxygens currently exist in the literature, giving a lithium−oxygen dimer minimum distance of 1.8 Å and a binding energy around −38 kcal/mol.[21,48] We carried out *ab initio* calculations for this dimer using the MP2 level of theory with the frozen core approximation and the Dunning aug-cc-pvtz basis set.[49] The NWChem computational package was used for these calculations.[50,51] The minimum dimer r_{Li-O} distance was 1.82 Å, and our force field gives a value of 1.81 Å in excellent agreement. However, the force field gives a binding energy that is too weak of −30.9 kcal/mol. This shows that good agreement between model and *ab initio* results were possible for the geometry, but the model underestimates the binding energy. The LJ parameters for the parametrized Li^+ model were $\sigma = 1.4$ Å and $\varepsilon = 0.4$ kcal/mol. One reason that the correct binding energy was not reproducible is due to neglecting many-body interactions. It should be noted that other force fields exist, some of which include many-body effects and all-atom models that have been shown to give excellent agreement with experiment for ionic conductivities.[21,52] The reason that a united-atom force field with fixed charges were used for this work is because we desired to carry out simulations with fairly high molecular weight polymers, in which MC simulations excel at their equilibration. However, MC simulations are inefficient at simulating polarizable molecular models. Also, the long simulation times for the described simulations (which are all 100 ns) may not be possible with our current computational resources with the use of many-body effects, which significantly increase the computational expense.

II.B. System Parameters. Three different types of systems were investigated: one with pure PEO LiTFSI (PURE), one with added ethylene carbonate (EC), and one with added propylene carbonate (PC). The simulations were set up with four PEO chains with a number-averaged molecular weight of 10 000 g/mol. The EO:Li ratio for the system was set to 15. In this work, comparisons where made with experimental values with much higher molecular weights (on the order of 500−600 K), but the molecular weight dependence on lithium diffusion has been found to level off around 10 000 g/mol. For instance, for a system of PEO with $LiCF_3SO_3$ with an EO:Li ratio of 20:1 at 90 °C, the lithium diffusion (D_{Li}) at molecular weights of 1000, 10 000, and 100 000 g/mol were found to be 5.0×10^{-7}, 1.0×10^{-7}, and 0.93×10^{-7} cm^2/s, respectively, showing a significant difference between the 1000 and 10 000 g/mol system of around a factor of 2, but only a 7% difference between 10 000 and 100 000 g/mol.[53] For the EC and PC systems, plasticizer was added until it reached 10 wt % (more on this later). All systems were equilibrated at 1 atm, and two temperatures were used, 348 and 320 K. The two temperatures were chosen because the lowest is 7 K above where PEO−LiTFSI (with EO:Li = 16) begins to crystallize,[54,55] and they allow comparisons between the entire range of temperatures found experimentally.[14] For quantitative agreement with experiment, higher temperatures would be desired, but the goal is to understand qualitative effects due to the addition of plasticizers. They all were placed in a periodic box with a LJ potential truncation of 9 Å employed, with analytical tail corrections. Long-ranged electrostatics were handled with the Ewald summation technique for the MC simulations[56] and the particle mesh Ewald summation technique for the MD simulations.[57] This combination (9 Å LJ cutoff) has been used to model many systems of ions in polar solvents.[58−60]

II.C. Monte Carlo Simulation Details. Monte Carlo simulations were all initiated with the LiTFSI ions placed on a square lattice and with four PEO polymers introduced in the system by growing them bead by bead utilizing configurational-bias Monte Carlo (CBMC).[61−64] The acceptance of these initial growth was governed by the first attempt that grew the whole molecule without overlapping with any neighboring molecules (not the regular Boltzmann acceptance). Following this initiation, the simulations were heated at 100 000 K for a short period of time, followed by slow cooling down to 320 or 348 K, depending on the system to study in the NVT ensemble. Following the cooling step, the system was inspected to make sure no salting out occurred, and then simulations were carried out in the NpT ensemble with an external pressure of 1 atm. The standard Metropolis MC translational and rotational moves were used for all of the molecules, and volume moves to equilibrate the pressure of the system in the NpT ensemble.[56] In addition, CBMC was used to equilibrate the configuration of $TFSI^-$ and the end segments of PEO. The CBMC reptation move was also used for PEO,[42] along with the SAFE-CBMC move for the equilibration of the structure of PEO interior segments.[65] Even with these MC moves, the equilibration of polymer structure with an average molecular weight of 10 000 g/mol is not achievable in the system described, and additional MC moves are required.[66] One set of moves designed for efficiently equilibrating long-chained polymer systems are the connectivity-altering Monte Carlo (CAMC) moves, which allow different polymer chains to exchange segments with one another.[67,68] One of these methods requires a certain degree of polydispersity for the polymers, which requires carrying out the simulations in the semigrand canonical ensemble. This has been used quite extensively for the investigation of polymers with CAMC simulations.[69] To accommodate the required polydispersity, an even distribution of polymer lengths between 75% of the average molecular weight to 125% was used, keeping the combined PEO molecular weight in the system fixed at 40 000 g/mol. A minimum of 100 000 MC cycles (one cycle being a total of N MC moves where N is the number of molecules in the system) of equilibration were carried out. After 100 000 MC cycles, the system energy and density was examined to make sure that it did not change between adjacent blocks of 20 000 MC cycles.

Simulations with plasticizers present were equilibrated by the following method. A liquid phase of EC or PC molecules (depending on the system) were brought into thermal equilibrium with the PEO phase utilizing the Gibbs ensemble Monte Carlo (GEMC) method. The GEMC method uses multiple simulation boxes with no explicit interface, but in thermal contact.[70−72] In GEMC, CBMC swap moves are used to equilibrate chemical potential between phases, and volume moves are used to equilibrate the volumes of the

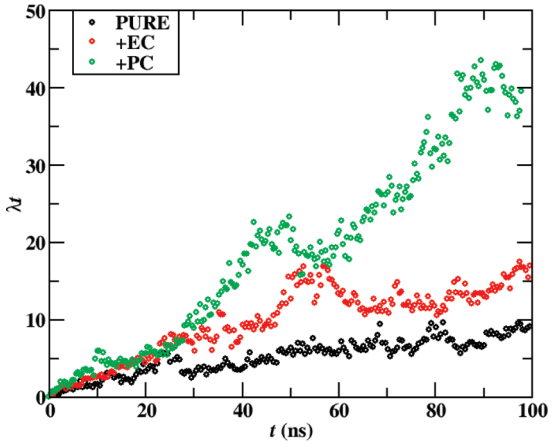

Figure 1. Curves used to calculate conductivity for the systems investigated at 320 K. The units for λt are S·ps/cm.

phases with an outside pressure bath. For our simulations, if allowed to equilibrate completely, the amount of plasticizer in the PEO phase would end up being much higher than 10 wt %; so to keep the plasticizer/PEO ratio at 10 wt %, no additional swap moves from the carbonate phase into the PEO phase were allowed after the wt % reached 10. An additional 50 000 MC cycles of equilibration were carried after this step.

II.D. Molecular Dynamics Simulation Details. After equilibration with the MC simulations, the coordinates were input into a MD simulation with velocities taken from the Boltzmann distribution. Following this, a total of 20 ns of equilibration in the NpT ensemble were carried out at the described temperatures (320 or 348 K) and 1 atm, in which the Berendsen thermostat was used.[73] The time step used in all MD simulations was set to 1 fs. Following the NpT equilibration, 100 ns production runs were carried out in the NVE ensemble to calculate all dynamical and structural properties. After equilibration, the simulation boxes had linear dimensions of approximately 40−43 Å depending on temperature and composition.

III. Results and Discussion

III.A. Conductivities. One of the goals of designing PEs is to maximize ionic conductivity which is important for battery operation. The calculations of ionic conductivity (λ) can be carried out with the Einstein relation by double summing over all ionic species (N)

$$\lambda = \lim_{t\to\infty} \frac{e^2}{6tVk_BT} \sum_{i=1}^{N}\sum_{j=1}^{N} z_i z_j \langle [\mathbf{R}_i(t) - \mathbf{R}_i(0)] \cdot [\mathbf{R}_j(t) - \mathbf{R}_j(0)] \rangle \quad (1)$$

where $\mathbf{R}_i(t)$ represents the vector position of species i at time t, the brackets denote the ensemble average, z_i and z_j are the ionic charges, V the volume, e the electron charge, k_B the Boltzmann constant, and T the temperature. To determine the conductivity, eq 1 without t has to be plotted as a function of t, which should be linear at long enough times (or as $t \to \infty$), and the slope of this linear region is the ionic conductivity. Figure 1 gives the plot used to calculate the conductivity for the systems at 320 K, essentially equal to the $\lambda \times t$, and Table 1 gives the conductivity calculated for all systems studied, along with sets of experimental data. Figure 1 shows that the curve used to calculate the conductivity is somewhat noisy, and as a result, the conductivity values have an uncertainty of up to 20%. For the PURE system, the calculation was extended to 200 ns (not shown), and the conductivity was found to stay relatively the same (within 10%) throughout that period. Multiple experimental values exist in the literature for the conductivity of PEO LiTFSI, but we found only one result for PEO LiTFSI with EC and PC. For the PURE system, there is a scatter in the experimental data, ranging from 6.31×10^{-4} to 15.1×10^{-4} S cm^{-1}. It should be noted that the EO:Li ratio in these also varies from 10 to 20, but there is little correlation between conductivities and EO:Li in this range. For instance, a previous study of a conductivity versus EO:Li ratio for an isotherm at 333 K of PEO−LiTFSI showed only a small change in the conductivity ranging between 5×10^{-4} and 7×10^{-4} throughout the span of 12−24 EO:Li ratio.[53] The spread in the experimental data shown in Table 1 is much larger than that, so the numbers probably depend on the experimental procedure and sample history.[74] The simulation results underestimate the values in comparison to experiment for the PURE system but appear to be within a factor of 2 of the experimental range. It has been argued that including polarizability in the molecular models will increase the conductivity,[21] and since our models do not include polarizability, which might be the underlying reason for the conductivity being lower than experiment. Nevertheless, the simulation results given here are reasonable. At the lower temperature of 320 K, the simulation results are within the range of experimental data, toward the lower end. In addition, the reduction in conductivity from 348 to 320 K is consistent between simulation and experiment, with the percentage reduction for the experiments ranging from 81% to 67%, and for the simulation, the reduction is 67%.

Table 1. Comparison of Conductivities (λ) for our Simulations Results and Experiments for the Ions and the Plasticizers

		T (K)	λ (10^{-4} S cm^{-1})
pure	sim	320	1.78
	expt[a]	320	1.4
	expt[b]	323	5.0
	expt[c]	320	1.8
	expt[d]	320	2.33
pure	sim	348	5.4
	expt[a]	348	6.31
	expt[b]	353	15.1
	expt[c]	348	9.5
	expt[d]	350	8.52
+PC	sim	320	3.92
	expt[b]	323	10.2
	sim	348	7.28
	expt[b]	353	19.5
+EC	sim	320	1.62
	expt[b]	323	10.96
	sim	348	7.87
	expt[b]	353	20.4

[a] Reference 55 for $(EO)_{10}$LiTFSI. [b] Reference 14 for $(EO)_{15}$LiTFSI. [c] Reference 77 for $(EO)_{16}$LiTFSI. [d] Reference 74 for $(EO)_{20}$LiTFSI.

With the addition of plasticizers, the conductivities at the higher temperatures increase by 35% for PC and 45% for EC for the simulations, showing the expected behavior of enhanced conductivity with the addition of plasticizers. The corresponding values for experiment are 29% for PC and 46% for EC.[14] While the absolute numbers do not have very good agreement with the results from this experiment (which is the highest of the experimental set), the consistency between the two is excellent, showing strong qualitative agreement.

III.B. Diffusion and Lithium Transference. Diffusion coefficients were calculated for each of the species, which are fairly straightforward in MD simulations using the

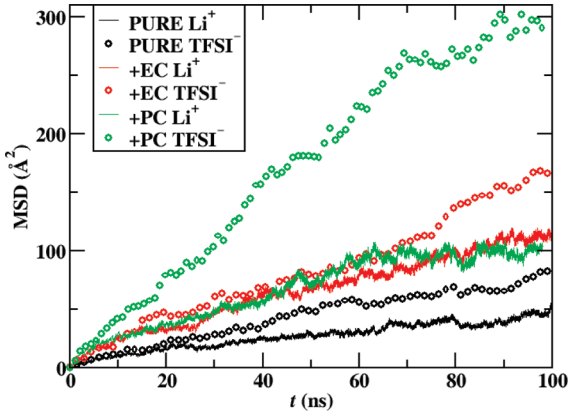

Figure 2. MSD of cations and anions for the systems investigated at 320 K.

Table 2. Comparison of τ_+ and D for Simulations Results and Experiments for the Ions and the Plasticizers in PEO

				D (10^{-8} cm^2 s^{-1})		
system		T (K)	τ_+	Li^+	$TFSI^-$	plasticizer
pure	sim	320	0.50	1.93	1.87	
	sim	348	0.337	3.10	6.10	
	expt[a]	348	0.487	14.2	14.9	
+PC	sim	320	0.252	1.91	5.68	24.9
	sim	348	0.239	3.93	12.5	82.7
	expt[a]	348	0.262	12.6	24.6	
+EC	sim	320	0.406	1.81	2.55	21.6
	sim	348	0.300	3.65	8.51	55.5
	expt[a]	348	0.381	17.2	25.3	

[a] Reference 14 for $(EO)_{15}$LiTFSI.

Einstein relation

$$D_i = \lim_{t\to\infty} \frac{\langle[\mathbf{R}_i(t) - \mathbf{R}_i(0)]^2\rangle}{6t} \tag{2}$$

where $\mathbf{R}_i(t)$ represents the vector position of species i at time t, and the brackets denote the ensemble average. Figure 2 gives the mean-square displacement (MSD), which is the quantity in the brackets in eq 2, as a function of time from the simulations for the lower of the two temperatures simulated (320 K). It can be observed that the curves are fairly linear after around 20 ns of simulation time. For the PURE system, the simulation times were extended 100−200 ns and were found to have the same slope as the previous 100 ns within the error of the calculation (results not shown). Apparently, it takes the system around 20 ns before the MSD increases in a linear fashion, and beyond that, the MSD appears to be fairly well behaved. These curves show a degree of noise not found in other simulation results,[21] but due to the lower temperatures used here (and overall lower values in MSD), our results are expected to be noisier. Using eq 2, the diffusion coefficients were calculated and are given in Table 2, along with experimental values for comparison. The uncertainties in the diffusion coefficients were estimated to be around 10%. In addition, a common property calculated to determine the quality of the electrolyte is lithium transference (τ_+)

$$\tau_+ = \frac{N_{Li} D_{Li}}{\sum_{ions} N_i D_i} = \frac{D_+}{D_+ + D_-} \tag{3}$$

where N_i is the number of ions of type i, but since the numbers of cations and anions are equal, the equation on the right is applicable. A higher lithium transference is often desirable for RLBs since it signals a higher proportion of the conductivity is due to lithium, and only lithium is oxidized and reduced at the electrodes. Along with the diffusion coefficients, τ_+ values are given in Table 2. We could not find experimental values for a system with an EO:Li ratio of 15 at 320 K. It should also be noted that the experimental values are based off an approximation of an ideal dilute solution, so they may not be quantitatively accurate[14] but should hold quite strongly for qualitative trends. Also, no uncertainties were given in the experimental results, but similar measurements were made of PEO−LiTFSI with an EO:Li ratio of 16 at 358 K and gave a value of approximately 0.41 ± 0.08.[75] This number is at a higher temperature than the one simulated in this work but provides a good baseline of the uncertainty and spread expected from the measurements. The simulation results are lower than experiment, but this is consistent throughout the range of systems investigated. For instance, the addition of plasticizers decreases τ_+, with the PC system showing the largest τ_+ decrease. Of interest is that when PC is added to the system, lithium diffusion remains relatively unchanged, and the $TFSI^-$ diffusion increases more dramatically. At the lower temperature of 320 K, the addition of plasticizers actually decreases lithium diffusion, while increasing $TFSI^-$ diffusion for both plasticizers. Also, the $TFSI^-$ diffusion increases to a greater degree for the PC system than the EC system. From these results, it is apparent that the addition of EC or PC plasticizers at this level may have little benefit for RLBs as most of the conductivity enhancements appear to be due to the anion, which is not what is oxidized and reduced at the electrodes. This is somewhat unexpected, as the diffusion coefficients for the plasticizers themselves (shown in Table 2) are much higher than any of the ionic species, by over an order of magnitude in many cases. If it would be possible for a lithium ion to strongly bind with one of the carbonates, it may have the ability to travel faster as a complex due to a vehicle mechanism, but this does not appear to be the case.

Table 3. Comparison of Conductivities, Diffusion Coefficients, and Degree of Dissociation (DOD) for the Ions in LITFSI and EC or PC

				D (10^{-6} cm^2 s^{-1})		
system		T (K)	λ (10^{-3} S cm^{-1})	Li^+	$TFSI^-$	DOD
EC	sim	313	5.1	1.0	1.3	0.64
	expt[a]	313	8.3	2.1	3.1	N/A
PC	sim	303	2.1	0.4	0.5	0.72
	expt[a]	303	5.2	1.6	2.1	0.62

[a] Reference 78.

In addition to the polymer systems, the diffusion coefficients and degree of dissociation (DOD) for LiTFSI in pure PC and EC were calculated using the described models, and the results are given in Table 3. The diffusion coefficients are lower than experiment by around a factor of 2−4, and the ionic conductivities were around a factor of 2 lower than experiment, which is consistent with the results for LiTFSI motion in the polymers. As was discussed for ionic conductivity in PEO−LiTFSI, the absence of polarizability is the likely reason the ionic diffusion is lower than experiment and is why if quantitative agreement with experiment is desired, using more computationally expensive polarizable models is probably necessary, as previous work with polarizable models have found better agreement for diffusion coefficients.[21,52] The DOD of LiTFSI is given in Table 3 for EC and PC and shows somewhat higher DODs than found experimentally for PC.

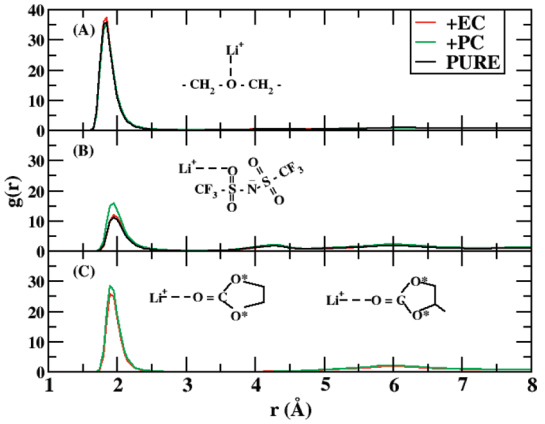

Figure 3. RDF at 320 K for lithium with (A) EO oxygens, (B) $TFSI^-$ oxygens, and (C) carbonate oxygens.

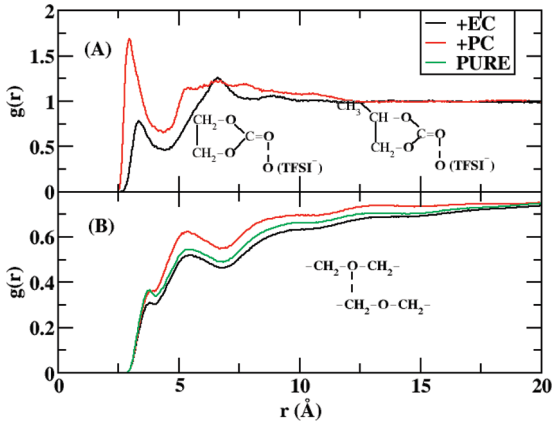

Figure 4. RDF at 320 K for (A) carbonate oxygens with $TFSI^-$ oxygens and (B) EO oxygens with EO methyl groups.

III.C. Structure. The structure of the system was investigated by calculating radial distribution functions (RDFs) of lithium with all oxygens that it had significant binding with. The RDFs between lithium and the oxygens for the systems investigated at 320 K are given in Figure 3. Lithium did not show significant binding with any other atoms than the ones shown. For instance, lithium did not coordinate with the sp^3 carbonyl oxygen (that is, bonded to two carbons) or the nitrogen atom in $TFSI^-$. The strength of coordination was highest with EO oxygens, slightly weaker with carbonate oxygens, and weakest with the $TFSI^-$ oxygens, as evidenced by the RDF peak height. This brings some insight into why the addition of plasticizers does not have a significant influence on lithium diffusion, as lithium will bind most strongly with EO oxygens. At the relatively modest concentrations of plasticizers in the system (10 wt %), EO oxygens are still dominant, and the addition of the weaker binding carbonate oxygens in the EC and PC systems does not appear to significantly alter the lithium−ether oxygen binding. The average first lithium−EO oxygen RDF peak is centered at a distance of 1.85 Å, and if the RDF is integrated with the number density over this first peak (up to 2.5 Å), the coordination number can be extracted. For the PURE system at 320 K, the lithium cation has a coordination number of 4.8 EO oxygens and 0.5 $TFSI^-$ oxygens, giving a total of 5.3. This has been investigated for a more concentrated salt system with an EO:Li ratio of 7.5, in which a coordination number of 4.9 ± 0.5 was found,[76] showing good agreement for a similar system. With the addition of plasticizers, little change in the distance or positions of the Li−EO RDF peak can be observed. However, with the addition of PC, lithium binds to a greater degree with the $TFSI^-$ oxygen, showing that PC may actually induce stronger interactions between lithium and $TFSI^-$. Multiple 20 ns blocks of simulations were compared to make sure that this was not due to statistical noise, and in all comparisons, the Li−O($TFSI^-$) increased with the addition of PC. What is somewhat unexpected is that the addition of EC has little to no effect on the Li−O($TFSI^-$) RDF, while PC does.

Figure 4 gives the RDF for carbonate oxygens with $TFSI^-$ oxygens and for EO oxygens with EO methylene groups. Interestingly, the PC oxygen appears to show a significant degree of binding with $TFSI^-$ oxygens (with a lithium ion bridging them), while EC oxygens show very little binding (more on this below) with these. The EO−EO oxygen−oxygen RDF shows stronger binding for the PC system and similar binding in the PURE and EC systems. A snapshot of a representative cluster from the PC system at 320 K

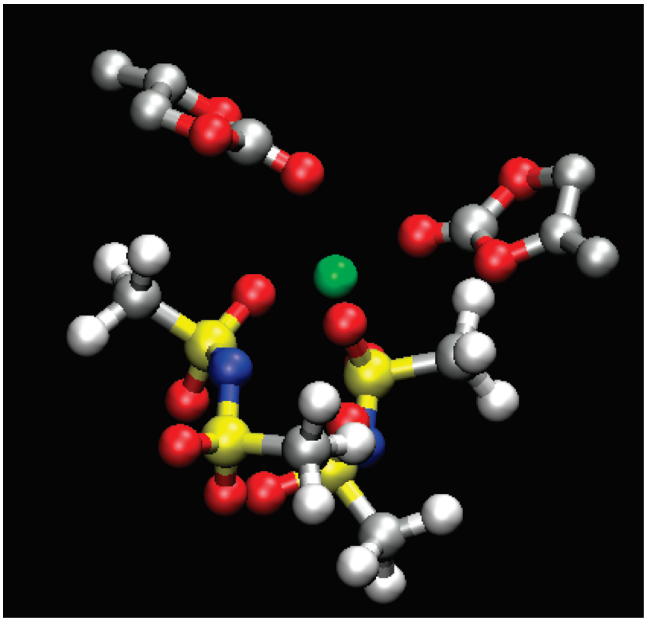

Figure 5. Snapshot of a cluster of molecules bound with the lithium ion, including two PC and two $TFSI^-$ molecules.

is shown in Figure 5, in which a single lithium ion and all non-PEO species (including PC and $TFSI^-$) bound with it are shown. PC binding with the lithium atom appears to induce interactions between lithium and $TFSI^-$. This is the origin of the higher first peak showed in the RDF between the PC and $TFSI^-$ oxygens. The methyl group in PC did not show any significant binding with any $TFSI^-$ atoms, with no high first RDF peaks between the atoms (not shown). However, the shape of PC appears to have a small effect on the ability of the system to form clusters of this type. This is evident in the RDFs, since EO groups bind the strongest in the PC system, and PC and $TFSI^-$ oxygens show a higher first peak due to their mutual binding with a lithium ion. Apparently, the methyl group in PC allows the formation of a structures in which clusters of lithium, PC, and $TFSI^-$ are embedded in the PEO. This is probably why the $TFSI^-$ diffusion increases to a greater degree in the PC system than the EC system. In contrast, the increase in lithium diffusion is very small, showing that there are a significant number of lithium ions in environments with slow diffusion.

Table 4 gives the coordination number (CN) of different oxygen species with lithium ions for the systems investigated

Table 4. Oxygen CN per Lithium Ion at 320 K

system	Li−O(EO)	Li−O(C=O)	Li−O(TFSI$^-$)	total CN
pure	4.84		0.59	5.43
EC	4.60	0.15	0.65	5.41
PC	4.43	0.18	0.69	5.30

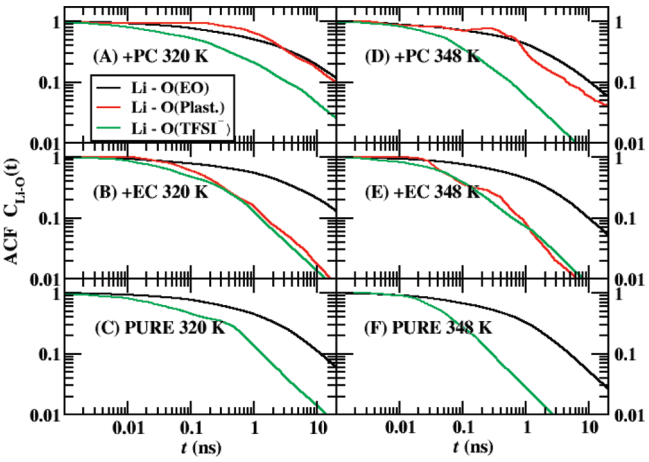

Figure 6. Residence time ACFs of Li$^+$ moving along PEO, EC/PC, and TFSI$^-$ for all simulations.

at 320 K. The reason for the rather small impact of the addition of plasticizers to lithium diffusion can be understood by the CNs, as lithium rarely coordinates with the carbonate oxygen, even though there are over twice as many PEO oxygens as carbonate oxygens. The addition of plasticizers increases the CN of TFSI$^-$ oxygens, especially with the addition of PC, as described previously. Taken as a whole, though, the binding of the carbonates is not strong enough with lithium to have a large effect on lithium diffusion.

III.D. Lithium Residence Times. There are generally two mechanisms that will be considered for lithium movement in PEO−LiTFSI with and without plasticizers. One is the movement of lithium hopping from one oxygen to the other, and the other is movement in a vehicular mechanism while lithium is bonded with either a plasticizer or TFSI$^-$. In order to better understand how the inclusion of plasticizers influence these mechanisms, the residence times were calculated for lithium with each oxygen it was found to strongly bind with. To calculate the lithium residence times, a time autocorrelation function (ACF) was calculated for lithium binding with each oxygen

$$C_{\mathrm{Li^+-O}}(t) = \frac{\langle H_{ij}(t)H_{ij}(0)\rangle}{\langle H_{ij}(0)H_{ij}(0)\rangle} \tag{4}$$

where $H_{ij}(t)$ is one if the ith Li$^+$ is coordinated with the jth oxygen atom and zero otherwise. A lithium was considered to be coordinated with an oxygen when their distance was less than 2.5 Å, which is near the minimums after the first lithium−oxygen RDF peaks. The ACF as a function of time is given in Figure 6 on a logarithmic scale. For the PURE systems, it is clear that binding with an EO oxygen lasts much longer than binding with TFSI$^-$, which is expected to a degree, as part of the reason TFSI$^-$ is chosen as a counterion for lithium is that it does not bind very strong with it. With the addition of EC, lithium appears to bind with EC oxygens to a similar degree as with TFSI$^-$, having its ACF falling off much faster than with an EO oxygen. In contrast, lithium binding with PC more closely follows the ACF of EO oxygens, and its ACF drops off much slower than with TFSI$^-$.

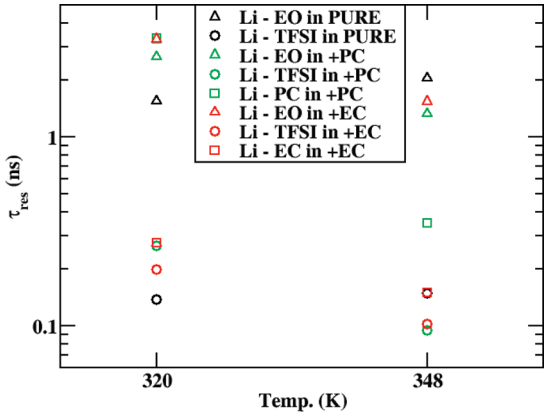

Figure 7. Comparison of total residence times of Li$^+$ with oxygens of EO, TFSI$^-$, and plasticizer (EC or PC) for all systems investigated.

The mean residence times themselves, τ_{res}, were calculated by fitting ACFs to $\exp[-(t/\tau_{res})^{\beta}]$, where β and τ_{res} were fit, with the results for τ_{res} given in Figure 7. The value of β ranged from 0.3 to 0.5. For all cases, the shortest τ_{res} is for lithium binding with TFSI$^-$, and the longest τ_{res} are with the EO oxygens for all cases. In between EO and TFSI$^-$ are the EC and PC oxygens, in which the longest residence time of the two is with PC oxygens. There is one exception to this trend, and that is of PC at 320 K, which has a similar residence time as EO, which is consistent with the ACF behavior that can be observed in Figure 6. Of interest is that the addition of plasticizers influences the τ_{res} values for lithium with EO oxygens, increasing τ_{res} at the lower temperature and decreasing them at the higher temperature. It should be noted that the EO τ_{res} in the PC system overlaps with the EO τ_{res} in the EC system. Again, as for τ_{res} with TFSI$^-$, adding plasticizer increases τ_{res} at 320 K and decreases τ_{res} at 348 K. It should be noted that for stronger confidence in these temperature dependencies more temperatures would have to be carried out than two to provide convincing evidence of a trend.

Apparently, the species lithium most strongly binds with are the EO oxygens, and overcoming this binding is what mostly promotes lithium mobility. The strongest effect the addition of plasticizers have on the systems appears to be how they influence lithium binding with EO oxygens, with shorter τ_{res} values after the addition of plasticizers at the higher temperature and longer τ_{res} values at the lower temperature. This is consistent with the lithium diffusion results calculated for the two temperatures, in which lithium diffusion increases at 348 K with the addition of plasticizers but decreases at 320 K.

III.E. Mechanism of Lithium Transport. To better understand the mechanism for lithium transport, the probability for a lithium ion to bind with one oxygen while bound with another was investigated. The hopping probability is given as follows

$$P(\mathrm{O}_i-\mathrm{O}_j) = \frac{N_{ij}}{\sum_i N_i} \tag{5}$$

where N_{ij} is the number of cases where a lithium bound with oxygen i *begins* to bind with oxygen j, and N_i are the total number of times when a lithium bound with an oxygen of type i *begins* to bind with any other oxygen. The definition for binding is when the lithium−oxygen distance is less than 2.5 Å. This hopping probability will be skewed to represent j oxygens that are the most concentrated in the system, which

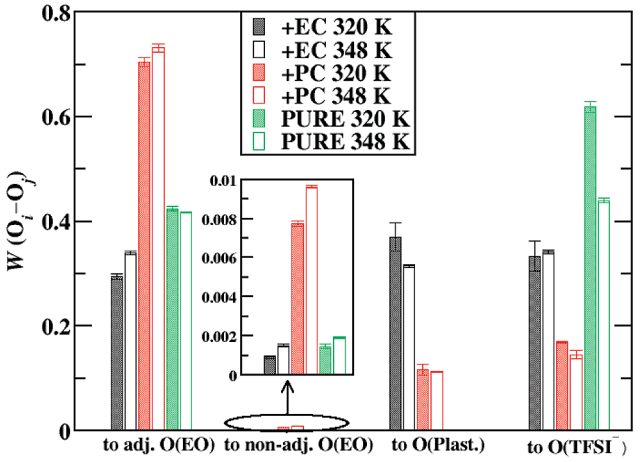

Figure 8. $W(O_i{-}O_j)$ for the systems investigated, where O_i is an EO oxygen.

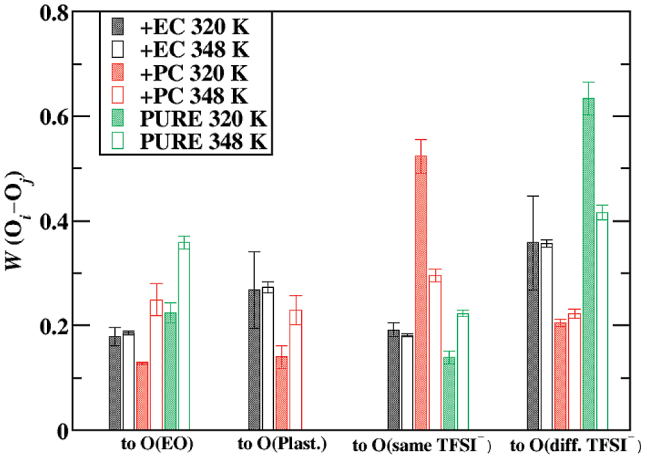

Figure 9. $W(O_i{-}O_j)$ for the systems investigated, where O_i is a $TFSI^-$ oxygen.

are the EO oxygens. To correct for this, we weighted the hopping probability by the ratio of oxygens of type *j* over all oxygens in the system

$$W(O_i - O_j) = \frac{P(O_i - O_j)}{N_j / \sum_k N_k} \tag{6}$$

where N_j represents the number of oxygens of type *j*. It should be noted that there are four oxygens per $TFSI^-$ ion, one per PEO repeat unit, and one per PC or EC (as only the carbonyl oxygen showed any binding).

Figure 8 gives $W(O_i{-}O_j)$ where O_i is an EO oxygen. It shows jumps to adjacent EO oxygens, nonadjacent EO oxygens (including those in another PEO chain), to carbonyl oxygens, and $TFSI^-$ oxygens. Of interest is that it is very rare for a lithium ion to jump to a nonadjacent PEO oxygen. This shows that the primary mechanism for movement along a PEO chain is along its longitudinal direction, even in an amorphous system. With the addition of both EC or PC, the probability to move to a $TFSI^-$ oxygen is reduced, which is expected, as the RDFs show stronger interactions with the carbonate oxygen than with a $TFSI^-$ oxygen. The jump probability to another PEO oxygen, though, increases dramatically with the addition of PC. This is not observed with the addition of EC. This result is not expected as the PC system has a higher first RDF peak for lithium with the $TFSI^-$ oxygen, and one would think that jumps to $TFSI^-$ oxygen would increase. However, this is consistent with the description given with the RDFs and the snapshot. If clusters with lithium in the center are formed in the PC systems, then it would be more difficult for a lithium ion bound to a PEO chain to transfer to a carbonate or $TFSI^-$ oxygen, since they will not be in as close of proximity.

Figure 9 shows the jump probability for a lithium from a $TFSI^-$ oxygen to other possible oxygens. The most probable transfer of a lithium ion is to another $TFSI^-$ oxygen, on either the same molecule or a different one. The addition of plasticizers decreases the probability to transfer to $TFSI^-$ oxygens of a different molecule and also decreases the probability of transferring to an EO oxygen. PC has the most pronounced effect, by promoting transfers between $TFSI^-$ oxygens on the same molecule. This is somewhat expected, as the addition of PC promotes stronger binding between lithium and $TFSI^-$ oxygens, as shown in the RDFs. Figure 10 shows the jump probability for a lithium from a carbonate oxygen to another oxygen. The PC system again

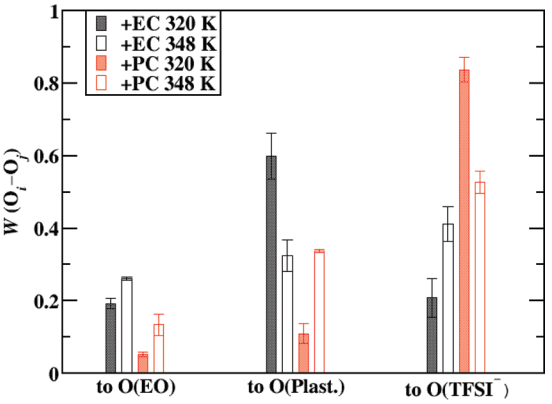

Figure 10. $W(O_i{-}O_j)$ for the systems investigated, where O_i is a carbonyl oxygen.

shows the highest probability to jump to a $TFSI^-$ oxygen, which is consistent with the previous results. The EC system shows differing behavior depending on the temperature of the system. At 320 K, the lithium jump probability is similar to all three oxygen types. At 348 K, lithiums are most likely to jump to another EC oxygen. In general, the addition of PC enhances lithium binding with $TFSI^-$ oxygens, and the probability to jump to one, which is not observed with the addition of EC to nearly the same degree.

III.F. Effect of Environment on Lithium Diffusion. The diffusion coefficients of lithium when bound to different oxygens defined as within a distance of 2.5 Å are shown in Figure 11. The diffusion coefficients were *not* calculated from 100 ns trajectories, but of much shorter 5 ns trajectories. Clearly this is too short of a time to estimate the true diffusion coefficient, but in general, fewer than 50% of the lithium−oxygen binding events lasted longer than 5 ns. As a result, 5 ns was chosen to get reasonable sampling and to allow *qualitative* comparisons to be made in diffusion coefficients. The $Li^+{-}EO$ values represent lithiums that are *only* bound to EO oxygens, while for plasticizer and $TFSI^-$ oxygens, the values are for lithium ions that are bound to them but can also be bound to other oxygens as well. This was done because the vast majority of lithium ions were bound to at least one EO oxygen. Examining the lithium ions bound to EO oxygens, it can be observed that the addition of PC slightly increases the diffusion of these oxygens, but the addition of EC has little effect. What is very interesting is that lithium ions bound to plasticizers do not show a significant

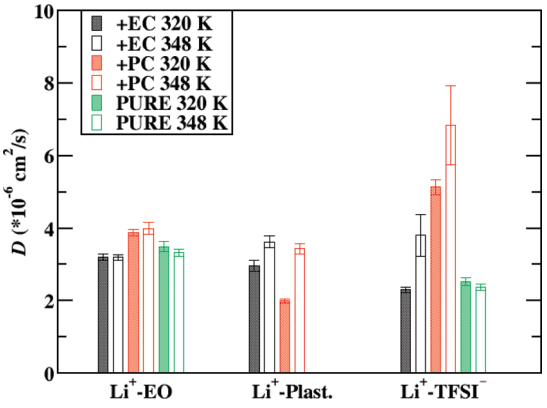

Figure 11. Apparent diffusion coefficients for lithium when bonded to different oxygens.

increase in diffusion and actually show a noticeable decrease for the PC system at 320 K. It should be noted that lithiums bound to plasticizers are almost always bound to EO oxygens as well, and the slower lithium diffusion is probably due to a cooperative effect between the PC and EO oxygens. For cases when lithium is bound with a $TFSI^-$ oxygen, unexpected results occur. In the PURE system, lithiums bound to $TFSI^-$ oxygens diffuse slower, while in the EC system, lithiums bound to $TFSI^-$ oxygens diffuse slower at 320 K and about the same, within the standard error, at 348 K. In contrast, for the PC system, lithium ions bound to $TFSI^-$ oxygens have much higher diffusion than in the other cases. This is expected, as for the PC system only, $TFSI^-$ diffusion is increased significantly, and it would be expected that lithiums bound with them would also have faster diffusion. This also brings some insight into how best to optimize lithium diffusion. For the case of LiTFSI, the binding of lithium with $TFSI^-$ is not very strong, so plasticizers need to bind strongly with lithium itself to facilitate faster diffusion. If another anion that binds stronger with lithium was used, enhancing the anion diffusion should additionally enhance the lithium diffusion as well.

IV. Conclusions

Molecular dynamics simulations, aided by connectivity-altering Monte Carlo simulations for equilibration, were used to understand how the addition of carbonate plasticizers influences ionic conduction and lithium transference for polymer electrolytes of LiTFSI in poly(ethylene oxide) with a number-averaged molecular weight of 10 000 g/mol. The results showed increases in ionic conductivity with addition of plasticizers, but fairly little increases in lithium diffusion, pointing to faster $TFSI^-$ diffusion as the main reason for the higher conductivity. The addition of propylene carbonate appeared to create domains that include clusters of propylene carbonate, lithium, and $TFSI^-$, increased the diffusion coefficient of $TFSI^-$, but also enhanced the binding between lithium and $TFSI^-$ oxygens, causing small increases in lithium diffusion. Future avenues for enhancing lithium diffusion in polymer electrolytes may focus on finding molecules that bind more strongly with lithium and allow the formation of faster moving clusters.

Acknowledgment. This research was funded by the Louisiana Board of Regents Research Competitiveness Subprogram contract 3LEQSF(2008-11)-RD-A-21. The calculations were carried out using the resources from the Louisiana Optical Network Initiative (LONI).

References and Notes

(1) Tarascon, J. M.; Armand, M. *Nature* **2001**, *414*, 359.
(2) Abraham, K. M. *Electrochim. Acta* **1993**, *38*, 1233.
(3) Attewell, A. *J. Power Sources* **1989**, *26*, 195.
(4) Balakrishnan, P. G.; Ramesh, R.; Prem Kumar, T. *J. Power Sources* **2006**, *155*, 401.
(5) Holzapfel, M.; Wursig, A.; Scheifele, W.; Vetter, J.; Novak, P. *J. Power Sources* **2007**, *174*, 1156.
(6) Spotnitz, R.; Franklin, J. *J. Power Sources* **2003**, *113*, 81.
(7) Gray, F. M. *Solid Polymer Electrolytes: Fundamentals and Technological Applications*; VCH Press: Cambridge, UK, 1991.
(8) Gauthier, M.; Belanger, A.; Kapfer, B.; Vassort, G.; Armand, M. *Polymer Electrolyte Reviews*; Elsevier Science Publishers: London, UK, 1989.
(9) Berthier, C.; Gorecki, W.; Minier, M.; Armand, M. B.; Chabagno, J. M.; Rigaud, P. *Solid State Ionics* **1983**, *11*, 91.
(10) Kumar, B.; Scanlon, L. G. *J. Electroceram.* **2000**, *5*, 127.
(11) Kerr, J. B. In *Lithium Batteries: Science and Technology*; Nazri, G., Pistoia, G., Eds.; Kluwer Academic Publishers: Boston, 2004; p 708.
(12) Gadjourova, Z.; Andreev, Y. G.; Tunstall, D. P.; Bruce, P. G. *Nature* **2001**, *412*, 520.
(13) Sun, X. G.; Liu, G.; Xie, J. B.; Han, Y. B.; Kerr, J. B. *Solid State Ionics* **2004**, *175*, 713.
(14) Kim, Y. T.; Smotkin, E. S. *Solid State Ionics* **2002**, *149*, 29.
(15) Kelly, I. E.; Owen, J. R.; Steele, B. C. H. *J. Power Sources* **1985**, *14*, 13.
(16) Munshi, M. Z. A.; Owens, B. B. *Solid State Ionics* **1988**, *26*, 41.
(17) Cameron, G. G.; Ingram, M. D.; Sarmouk, K. *Eur. Polym. J.* **1990**, *26*, 1097.
(18) Huq, R.; Farrington, G. C.; Koksbang, R.; Tonder, P. E. *Solid State Ionics* **1992**, *57*, 277.
(19) Klein, R. J.; Runt, J. *J. Phys. Chem. B* **2007**, *111*, 13188.
(20) Borodin, O.; Smith, G. D. *Macromolecules* **2006**, *39*, 1620.
(21) Borodin, O.; Smith, G. D. *J. Phys. Chem. B* **2006**, *110*, 6293.
(22) Hyun, J. K.; Dong, H.; Rhodes, C. P.; Frech, R.; Wheeler, R. A. *J. Phys. Chem. B* **2001**, *105*, 3329.
(23) Müller-Plathe, F.; Van Gunsteren, W. F. *J. Chem. Phys.* **1995**, *103*, 4745.
(24) Neyertz, S.; Brown, D. *J. Chem. Phys.* **1996**, *104*, 3797.
(25) Borodin, O.; Smith, G. D.; Douglas, R. *J. Phys. Chem. B* **2003**, *107*, 6824.
(26) Siqueira, L. J. A.; Ribeiro, M. C. C. *J. Chem. Phys.* **2006**, 125.
(27) Boinske, P. T.; Curtiss, L.; Halley, J. W.; Lin, B.; Sutjianto, A. *J. Comput.-Aided Mater. Des.* **1996**, *3*, 385.
(28) Duan, Y.; Halley, J. W.; Curtiss, L.; Redfern, P. *J. Chem. Phys.* **2005**, *122*, 1.
(29) Brandell, D.; Liivat, A.; Aabloo, A.; Thomas, J. O. *J. Mater. Chem.* **2005**, *15*, 4338.
(30) Borodin, O.; Smith, G. D. *J. Solution Chem.* **2007**, *36*, 803.
(31) Borodin, O.; Smith, G. D. *Macromolecules* **1998**, *31*, 8396.
(32) Catlow, C. R. A.; Mills, G. E. *Electrochim. Acta* **1995**, *40*, 2057.
(33) Forsyth, M.; Payne, V. A.; Ratner, M. A.; de Leeuw, S. W.; Shriver, D. F. *Solid State Ionics* **1992**, *53−56*, 1011.
(34) Payne, V. A.; Lonergan, M. C.; Forsyth, M.; Ratner, M. A.; Shriver, D. F.; de Leeuw, S. W.; Perram, J. W. *Solid State Ionics* **1995**, *81*, 171.
(35) Neyertz, S.; Brown, D.; Thomas, J. O. *J. Chem. Phys.* **1994**, *101*, 10064.
(36) Xie, L.; Farrington, G. C. *Solid State Ionics* **1992**, *53−56*, 1054.
(37) Xie, L.; Farrington, G. C. *Solid State Ionics* **1993**, *60*, 19.
(38) Borodin, O.; Smith, G. D. *J. Phys. Chem. B* **2009**, *113*, 1763.
(39) Borodin, O.; Smith, G. D. *J. Phys. Chem. B* **2006**, *110*, 4971.
(40) Brandell, D.; Kasemägi, H.; Aabloo, A. *Electrochim. Acta*, in press.
(41) Hunt, A.; Punning, A.; Anton, M.; Aabloo, A.; Kruusmaa, M. **2008**; Vol. *6927*.
(42) Wick, C. D.; Theodorou, D. N. *Macromolecules* **2004**, *37*, 7026.
(43) Stubbs, J. M.; Potoff, J. J.; Siepmann, J. I. *J. Phys. Chem. B* **2004**, *108*, 17596.
(44) Chen, B.; Potoff, J. J.; Siepmann, J. I. *J. Phys. Chem. B* **2002**, *105*, 3093.
(45) Canongia Lopes, J. N.; Deschamps, J.; Pádua, A. A. H. *J. Phys. Chem. B* **2004**, *108*, 2038.
(46) Wick, C. D.; Siepmann, J. I.; Theodorou, D. N. *J. Am. Chem. Soc.* **2005**, *127*, 12338.
(47) Cornell, W. D.; Cieplak, P.; Bayly, C. I.; Gould, I. R.; Merz, K. M.; Ferguson, D. M.; Spellmeyer, D. C.; Fox, T.; Caldwell, J. W.; Kollman, P. A. *J. Am. Chem. Soc.* **1995**, *117*, 5179.
(48) Sutjianto, A.; Curtiss, L. A. *J. Phys. Chem. A* **1998**, *102*, 968.
(49) Boys, S. F.; Bernardi, F. *Mol. Phys.* **1970**, *19*, 553.

(50) Kendall, R. A.; Apra, E.; Bernholdt, D. E.; Bylaska, E. J.; Dupuis, M.; Fann, G. I.; Harrison, R. J.; Ju, J. L.; Nichols, J. A.; Nieplocha, J.; Straatsma, T. P.; Windus, T. L.; Wong, A. T. *Comput. Phys. Commun.* **2000**, *128*, 260.
(51) Bylaska, E. J.; et al. NWChem version 5.0, **2006**.
(52) Borodin, O.; Smith, G. D. *J. Phys. Chem. B* **2006**, *110*, 6279.
(53) Lascaud, S. University of Montreal, **1996**.
(54) Marzantowicz, M.; Dygas, J. R.; Krok, F.; Nowiński, J. L.; Tomaszewska, A.; Florjańczyk, Z.; Zygadło-Monikowska, E. *J. Power Sources* **2006**, *159*, 420.
(55) Marzantowicz, M.; Dygas, J. R.; Krok, F.; Florjańczyk, Z.; Zygadło-Monikowska, E. *J. Non-Cryst. Solids* **2007**, *353*, 4467.
(56) Allen, M. P.; Tildesley, D. J. *Computer Simulation of Liquids*; Oxford University Press: Oxford, 1987.
(57) Essmann, U.; Perera, L.; Berkowitz, M. L.; Darden, T.; Lee, H.; Pedersen, L. G. *J. Chem. Phys.* **1995**, *103*, 8577.
(58) Chang, T. M.; Dang, L. X. *Chem. Rev.* **2006**, *106*, 1305.
(59) Jungwirth, P.; Tobias, D. *J. Chem. Rev.* **2006**, *106*, 1259.
(60) Jensen, K. P.; Jorgensen, W. L. *J. Chem. Theory Comput.* **2006**, *2*, 1499.
(61) Siepmann, J. r. I. *Mol. Phys.* **1990**, *70*, 1145.
(62) Siepmann, J. I.; Frenkel, D. *Mol. Phys.* **1992**, *75*, 59.
(63) De Pablo, J. J.; Laso, M.; Suter, U. W. *J. Chem. Phys.* **1992**, *96*, 6157.
(64) Frenkel, D.; Mooij, G. C. A. M.; Smit, B. *J. Phys.: Condens. Matter* **1992**, *4*, 3053.
(65) Wick, C. D.; Siepmann, J. I. *Macromolecules* **2000**, *33*, 7207.
(66) Auhl, R.; Everaers, R.; Grest, G. S.; Kremer, K.; Plimpton, S. J. *J. Chem. Phys.* **2003**, *119*, 12718.
(67) Pant, P. V. K.; Theodorou, D. N. *Macromolecules* **1995**, *28*, 7224.
(68) Karayiannis, N. C.; Mavrantzas, V. G.; Theodorou, D. N. *Phys. Rev. Lett.* **2002**, 88.
(69) Mavrantzas, V. G.; Boone, T. D.; Zervopoulou, E.; Theodorou, D. N. *Macromolecules* **1999**, *32*, 5072.
(70) Panagiotopoulos, A. Z. *Mol. Phys.* **1987**, *61*, 813.
(71) Panagiotopoulos, A. Z. *Mol. Simul.* **1992**, *9*, 1.
(72) Smit, B.; De Smedt, P.; Frenkel, D. *Mol. Phys.* **1989**, *68*, 931.
(73) Berendsen, H. J. C.; Postma, J. P. M.; Vangunsteren, W. F.; Dinola, A.; Haak, J. R. *J. Chem. Phys.* **1984**, *81*, 3684.
(74) Volel, M.; Armand, M.; Gorecki, W. *Macromolecules* **2004**, *37*, 8373.
(75) Edman, L.; Doeff, M. M.; Ferry, A.; Kerr, J.; De Jonghe, L. C. *J. Phys. Chem. B* **2000**, *104*, 3476.
(76) Mao, G.; Saboungi, M. L.; Price, D. L.; Armand, M. B.; Howells, W. S. *Phys. Rev. Lett.* **2000**, *84*, 5536.
(77) Sylla, S.; Sanchez, J. Y.; Armand, M. *Electrochim. Acta* **1992**, *37*, 1699.
(78) Hayamizu, K.; Aihara, Y.; Arai, S.; Martinez, C. G. *J. Phys. Chem. B* **1999**, *103*, 519.